Brief Report

Soluble FLT1 Gene Therapy Alleviates Brain Arteriovenous Malformation Severity

Wan Zhu, PhD; Fanxia Shen, MD*; Lei Mao, MD, PhD*; Lei Zhan, BS; Shuai Kang, MD; Zhengda Sun, MD, PhD; Jeffrey Nelson, MS; Rui Zhang, PhD; Dingquan Zou, MD; Cameron M. McDougall, MD; Michael T. Lawton, MD; Thiennu H. Vu, MD, PhD; Zhijian Wu, PhD; Abraham Scaria, PhD; Peter Colosi, PhD; John Forsayeth, PhD; Hua Su, MD

Background and Purpose—Brain arteriovenous malformation (bAVM) is an important risk factor for intracranial hemorrhage. Current therapies are associated with high morbidities. Excessive vascular endothelial growth factor has been implicated in bAVM pathophysiology. Because soluble FLT1 binds to vascular endothelial growth factor with high affinity, we tested intravenous delivery of an adeno-associated viral vector serotype-9 expressing soluble FLT1 (AAV9-sFLT1) to alleviate the bAVM phenotype.

Methods—Two mouse models were used. In model 1, bAVM was induced in R26CreER;*Eng*$^{2f/2f}$ mice through global *Eng* gene deletion and brain focal angiogenic stimulation; AAV2-sFLT02 (an AAV expressing a shorter form of sFLT1) was injected into the brain at the time of model induction, and AAV9-sFLT1, intravenously injected 8 weeks after. In model 2, SM22αCre;*Eng*$^{2f/2f}$ mice had a 90% occurrence of spontaneous bAVM at 5 weeks of age and 50% mortality at 6 weeks; AAV9-sFLT1 was intravenously delivered into 4- to 5-week-old mice. Tissue samples were collected 4 weeks after AAV9-sFLT1 delivery.

Results—AAV2-sFLT02 inhibited bAVM formation, and AAV9-sFLT1 reduced abnormal vessels in model 1 (GFP versus sFLT1: 3.66±1.58/200 vessels versus 1.98±1.29, $P<0.05$). AAV9-sFLT1 reduced the occurrence of bAVM (GFP versus sFLT1: 100% versus 36%) and mortality (GFP versus sFLT1: 57% [12/22 mice] versus 24% [4/19 mice], $P<0.05$) in model 2. Kidney and liver function did not change significantly. Minor liver inflammation was found in 56% of AAV9-sFLT1–treated model 1 mice.

Conclusions—By applying a regulated mechanism to restrict sFLT1 expression to bAVM, AAV9-sFLT1 can potentially be developed into a safer therapy to reduce the bAVM severity. **(*Stroke*. 2017;48:00-00. DOI: 10.1161/STROKEAHA.116.015713.)**

Key Words: angiogenesis ■ animals ■ brain ■ gene therapy

Brain arteriovenous malformations (bAVMs) tend to rupture spontaneously causing intracranial hemorrhage. Current treatments are associated with high morbidities/mortalities. New, effective, and safe therapies are, therefore, needed.

Vascular endothelial growth factor (VEGF) is abnormally high in bAVM lesions.[1] Patients with an autosomal dominant disease, Hereditary Hemorrhagic Telangiectasia, have a higher incidence of AVMs in multiple organs, including the brain. Increased VEGF has also been found in Hereditary Hemorrhagic Telangiectasia patients' plasma.[2] Therefore, inhibiting VEGF may be effective to treat bAVM. However, considerable side effects are associated with commonly used blocking agents: VEGF antibodies[3] and tyrosine kinase inhibitors.[4]

Soluble FMS-like tyrosine kinase 1 (sFLT1) contains only the extracellular domains of FLT1 (VEGFR1) and binds with VEGF.[5]

The adeno-associated virus (AAV) mediates long-term transgene expression in nondividing cells. AAV serotype-9 (AAV9) passes through the blood–brain barrier around the angiogenic region.[6] Intravenous injection of AAV9-sFLT1 inhibits VEGF-induced brain angiogenesis.[6]

Our study shows that through intrabrain or intravenous injection, AAV-sFLT1 attenuates bAVM phenotypes.

Received October 12, 2016; final revision received January 5, 2017; accepted January 23, 2017.

From the Center for Cerebrovascular Research, Department of Anesthesia and Perioperative Care (W.Z., F.S., L.Z., S.K., J.N., R.Z., D.Z., H.S.), Department of Neurological Surgery (L.M., C.M.M., M.T.L., J.F.), Department of Radiology (Z.S.), and Department of Medicine (T.H.V.), University of California, San Francisco; Ocular Gene Therapy Core, National Eye Institute, National Institutes of Health, Bethesda, MD (Z.W.); Sanofi-Genzyme R&D Center, Framingham, MA (A.S.); and BioMarin Pharmaceutical Inc, Novato, CA (P.C.).

The online-only Data Supplement is available with this article at http://stroke.ahajournals.org/lookup/suppl/doi:10.1161/STROKEAHA.116.015713/-/DC1.

*Drs Shen and Mao contributed equally.

Correspondence to Hua Su, MD, Department of Anesthesia and Perioperative Care, University of California, San Francisco, 1001 Potrero Ave Box 1363, San Francisco, CA 94143. E-mail: hua.su@ucsf.edu

Methods

Animals

The Institutional Animal Care and Use Committee of the University of California, San Francisco approved protocol/experimental procedures. Institutional Animal Care and Use Committee and Animal Care Facility staff provided animal husbandry.

Eng$^{2f/2f}$ (*Endoglin*, Hereditary Hemorrhagic Telangiectasia–causative gene) mice[7] were crossbred with R26CreER or SM22αCre mice (Jackson Laboratory, Bar Harbor, ME) to produce R26CreER;*Eng*$^{2f/2f}$ or SM22αCre;*Eng*$^{2f/2f}$ mice.

In model 1, 8-week-old R26CreER;*Eng*$^{2f/2f}$ mice were intraperitoneally injected with tamoxifen (2.5 mg/25g of body weight) daily for 3 consecutive days to globally delete the *Eng* gene, and intrabrain injected with AAV1-VEGF to induce focal angiogenesis when the first dose of tamoxifen was given; bAVM developed 8 weeks later.[8] AAV1-sFLT02 was coinjected with AAV1-VEGF at the time of model induction, and AAV9-sFLT1, intravenously injected 8 weeks after.

In model 2, SM22αCre;*Eng*$^{2f/2f}$ mice were used. AAV9-sFLT1 was intravenously injected to 4- to 5-week-old mice.

Random group assignment was applied, and treatment end point selected based on a previous study.[6]

Statistics

Sample sizes are shown in the figures. GraphPad Prism 6 was used to analyze data, *t* test for comparing 2 groups, and 2-way ANOVA with Tukey correction for >2 groups with multiple comparisons. Survival rate was analyzed using log-rank test. Data are presented as mean±SD. *P* value <0.05 was considered statistically significant. All methods are described in the online-only Data Supplement.

Results

To test whether sFLT1 inhibits bAVM formation, AAV2-sFLT02 containing the VEGF-binding domain 2 of human sFLT1 and a CH3 domain of IgG1[6] was coinjected with AAV1-VEGF into the brain of model 1 mice when the first dose of tamoxifen was given. Eight weeks later, cerebrovasculature was latex cast (Figure IA and IB in the online-only Data Supplement). Because of size, latex particles enter the veins only when there is an arteriovenous shunt (an AVM hallmark). bAVMs were detected in AAV2-EV (empty vector)–treated mice, but not in AAV2-sFLT02–treated mice (Figure 1A). AAV2-sFLT02–treated mice had a smaller latex-perfused area than AAV2-EV–injected mice (*P*=0.037; Figure 1B; Figure IC in the online-only Data Supplement), indicating that sFLT02 inhibited bAVM formation.

To reduce risk of intralesion injection, AAV9-sFLT1 expressing a full-length human sFLT1[6] or AAV9-GFP (green fluorescent protein, control) was intravenously delivered to model 1 mice 8 weeks after model induction when bAVM had developed (Figure IIA and IIB in the online-only Data Supplement).[8] Gene expression in bAVM was confirmed via histological analysis for GFP and ELISA for sFLT1 (Figure IIC through IIE in the online-only Data Supplement).

Four weeks later, therapeutic effect was evaluated by analyzing vessel density and dysplasia vessels (dysplasia index: number of vessels larger than 15 μm/200 vessels)[8] using fresh-frozen brain sections (Figure IIB in the online-only Data Supplement). Compared with AAV9-GFP–treated mice (3.66±1.58), AAV9-sFLT1–treated mice had a lower dysplasia index (1.98±1.29, *P*=0.011) and a trend toward lower vessel density (*P*=0.17; Figure 2), indicating that AAV9-sFLT1 reduced bAVM severity. No GFP signal was detected in the fresh-frozen sections of Ad-GFP–injected brain (Figure III in the online-only Data Supplement). The positive signals of fluorescent-labeled lectin and CD31 antibody staining were completely colocalized (Figure IIIB in the online-only Data Supplement).

To confirm that the effect in model 1 was not because of inhibition of exogenous VEGF used to induce bAVM, we tested AAV9-sFLT1 in model 2, in which bAVMs develop spontaneously without exogenous VEGF stimulation. AAV9-sFLT1 was intravenously injected into 4- to 5-week-old mice (Figure IVA in the online-only Data Supplement) because 90% of model 2 mice had bAVMs by 5 weeks and 50% died by 6 weeks.[8] About 57% of AAV9-GFP–treated and 24% of AAV9-sFLT1–treated mice died during the 4-week treatment period (*P*=0.036; Figure 3A; Table I in the online-only Data Supplement). All AAV9-GFP–treated mice had bAVM; only 36% of AAV9-sFLT1–treated mice had detectable bAVMs (Figure 3B and 3C; Figure IVB through IVD). Therefore, AAV9-sFLT1 treatment also reduced the severity of spontaneously developed bAVM.

Potential adverse effects on the liver and kidney were analyzed. The activities of alkaline phosphatase and alanine transaminase and the levels of creatinine were similar in AAV9-GFP–treated, AAV9-sFLT1–treated, and untreated groups in model 1 (Figure VA through VC in the online-only Data Supplement). Small clusters of inflammatory cells (including monocytes and lymphocytes) were detected in the liver of 58% of AAV9-GFP–treated and 56% of AAV9-sFLT1–treated mice, but not in AAV9-EV–injected mice (Figure VD and VE in the online-only Data Supplement; Table II in the online-only Data Supplement). Body weight of AAV9-sFLT1–treated

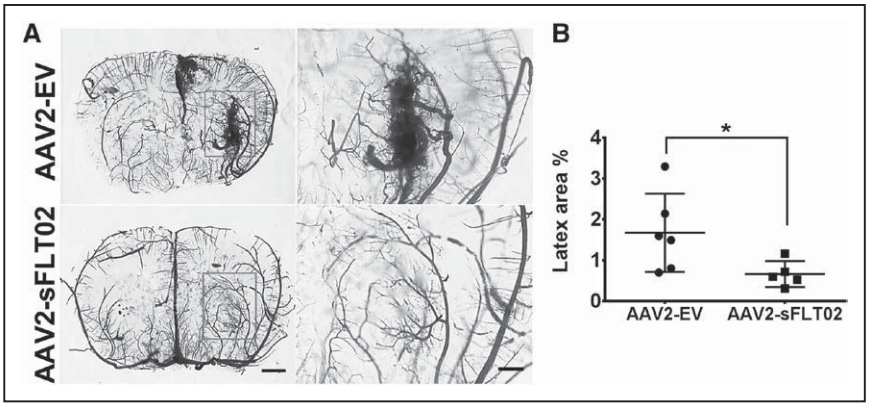

Figure 1. AAV2-sFLT02 in situ inhibits brain arteriovenous malformations (bAVM) in model 1 (R26CreER;*Eng*$^{2f/2f}$). **A,** Representative images: coronal sections—latex-perfused brain. AVM developed in angiogenic regions (rectangles) of adeno-associated viral vector serotype-2 (AAV2)-EV–injected but not in AAV2-sFLT02–injected mice. Right: Close-up views: angiogenic region. Scale bars: 1 mm (left) or 500 μm (right). **B,** Latex-perfused area quantification. AAV2-EV group: n=6. AAV2-sFLT02 group: n=5. **P*=0.037.

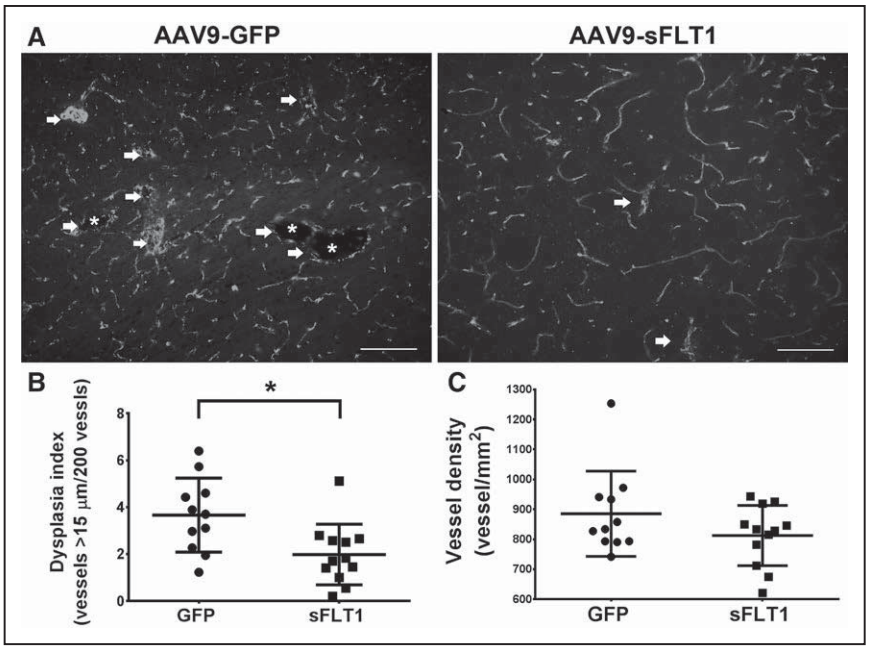

Figure 2. Adeno-associated viral vector serotype-9 expressing soluble FLT1 (AAV9-sFLT1) intravenously reduces the dysplasia index in brain arteriovenous malformation (bAVM) in model 1 (R26CreER;*Eng*$^{2f/2f}$). **A**, Representative CD31 antibody-stained brain images. White arrows: Abnormal vessels. White stars: Enlarged abnormal vessel lumens. Scale bar=100 μm. **B**, Dysplasia index quantifications. **C**, Vessel density quantifications. GFP-treated group: n=11. sFLT1-treated group: n=12. **P*=0.011.

R26CreER;*Eng*$^{2f/2f}$ mice did not increase as much as control mice during the treatment period and was lower than the control groups at the end of therapy (*P*=0.044; Figure VI in the online-only Data Supplement).

Discussion

We tested an antiangiogenic gene therapy to treat bAVM in (1) VEGF-induced adult onset model and (2) spontaneously developed model. We showed that in situ injection of AAV1-sFLT02 at the time of model induction inhibited bAVM formation in model 1; intravenously delivered AAV9-sFLT1 reduced bAVM severity in both models.

VEGF functions mainly through VEGFR1 (or FLT1) and VEGFR2. Whereas VEGFR2 is known to mediate endothelial cell mitosis and vascular permeability, VEGFR1-mediated signaling is complex and context dependent. VEGF–VEGFR1 signaling also induces monocytes homing to the injured tissue. sFLT1 effect most likely occurs when it binds to excessive VEGF in the brain parenchyma, thus quenching VEGF signaling through membrane-bound receptors. We found that sFLT1 overexpression reduced dysplasia vessels, with no significant reduction of CD68$^+$ cells in the bAVM (data not shown), suggesting that therapeutic effect might be achieved by reducing VEGFR2 signaling. Although we were not able to quantify the number of dysplasia vessels in model 2 because of the unpredictable lesion locations, AAV9-sFLT1 reduced mortality and the presence of bAVM in this model, suggesting that the effect observed in model 1 was not merely through exogenous VEGF inhibition. Future studies will be needed to determine the underlying mechanisms.

Bevacizumab (Avastin) treatment in an adult onset *Alk1*-deficient model reduced bAVM severity.[9] However, bevacizumab causes bilateral pulmonary embolisms, thrombosis, and hypertension in Hereditary Hemorrhagic Telangiectasia patients.[3] Although intravenously delivered AAV9-sFLT1 caused weight loss and liver inflammation, AAV9-EV did not. Therefore, the side effects were caused by constitutive sFLT1 expression. An antitumor study showed ascites and kidney damage in mice treated with adenoviral vector expressing sFLT1 constitutively, but not in mice treated with intermittent

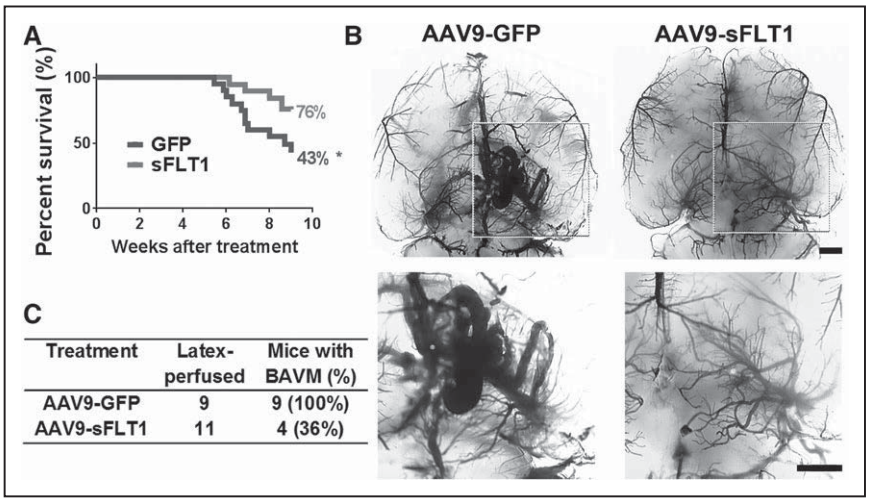

Figure 3. Adeno-associated viral vector serotype-9 expressing soluble FLT1 (AAV9-sFLT1) intravenously reduces spontaneously developed brain arteriovenous malformation (bAVM) in model 2 (SM22αCre;*Eng*$^{2f/2f}$). **A**, Survival curves. GFP and sFLT1: AAV9-GFP and AAV9-sFLT1 injection. **P*=0.036. **B**, Representative latex cast brain images. **Top**, Clarified brain. **Bottom**, Close-up views. Scale bars=1 mm. **C**, bAVM rates.

sFLT1 expression,[10] indicating that sFLT1 side effects can be reduced by controlling expression. An AAV gene therapy has been approved recently, and many clinical trials are ongoing.[11] AAV gene therapy could be developed into a safer and an effective therapy to treat chronic diseases such as AVM.

Although our mouse models have many key characteristics of human bAVM,[12] no hemodynamic changes in the AV fistula and the nearby brain–blood vessels have been studied. However, our findings suggest that AAV-sFLT1 could be developed into a minimally invasive and safe antiangiogenesis gene therapy for bAVM. Minor adverse effects could be minimized by controlling sFLT1 expression.

Sources of Funding

This study was supported by research grants from the National Institutes of Health (R01 NS027713, R01 HL122774, and R21 NS083788), the Michael Ryan Zodda Foundation, and University of California, San Francisco Research Evaluation and Allocation Committee (REAC) to Dr Su and by a Young Investigator Award from Cure HHT (Hereditary Hemorrhagic Telangiectasia) Foundation to Dr Zhu.

Disclosures

None.

References

1. Hashimoto T, Wu Y, Lawton MT, Yang GY, Barbaro NM, Young WL. Coexpression of angiogenic factors in brain arteriovenous malformations. *Neurosurgery*. 2005;56:1058–1065; discussion 1058.
2. Sadick H, Riedel F, Naim R, Goessler U, Hörmann K, Hafner M, et al. Patients with hereditary hemorrhagic telangiectasia have increased plasma levels of vascular endothelial growth factor and transforming growth factor-beta1 as well as high ALK1 tissue expression. *Haematologica*. 2005;90:818–828.
3. Tabouret T, Gregory T, Dhooge M, Brezault C, Mir O, Dréanic J, et al. Long term exposure to antiangiogenic therapy, bevacizumab, induces osteonecrosis. *Invest New Drugs*. 2015;33:1144–1147. doi: 10.1007/s10637-015-0283-x.
4. Orphanos GS, Ioannidis GN, Ardavanis AG. Cardiotoxicity induced by tyrosine kinase inhibitors. *Acta Oncol*. 2009;48:964–970. doi: 10.1080/02841860903229124.
5. Chung AS, Ferrara N. Developmental and pathological angiogenesis. *Annu Rev Cell Dev Biol*. 2011;27:563–584. doi: 10.1146/annurev-cellbio-092910-154002.
6. Shen F, Mao L, Zhu W, Lawton MT, Pechan P, Colosi P, et al. Inhibition of pathological brain angiogenesis through systemic delivery of AAV vector expressing soluble FLT1. *Gene Ther*. 2015;22:893–900. doi: 10.1038/gt.2015.57.
7. Allinson KR, Carvalho RL, van den Brink S, Mummery CL, Arthur HM. Generation of a floxed allele of the mouse Endoglin gene. *Genesis*. 2007;45:391–395. doi: 10.1002/dvg.20284.
8. Choi EJ, Chen W, Jun K, Arthur HM, Young WL, Su H. Novel brain arteriovenous malformation mouse models for type 1 hereditary hemorrhagic telangiectasia. *PLoS One*. 2014;9:e88511. doi: 10.1371/journal.pone.0088511.
9. Walker EJ, Su H, Shen F, Degos V, Amend G, Jun K, et al. Bevacizumab attenuates VEGF-induced angiogenesis and vascular malformations in the adult mouse brain. *Stroke*. 2012;43:1925–1930. doi: 10.1161/STROKEAHA.111.647982.
10. Sivanandam VG, Stephen SL, Hernandez-Alcoceba R, Alzuguren P, Zabala M, van Rooijen N, et al. Lethality in an anti-angiogenic tumor gene therapy model upon constitutive but not inducible expression of the soluble vascular endothelial growth factor receptor 1. *J Gene Med*. 2008;10:1083–1091. doi: 10.1002/jgm.1244.
11. Pollack A. European agency backs approval of a gene therapy. *New York Times (New York Edition)*. 2012;July 21:Sect B (Health):B1.
12. Walker EJ, Su H, Shen F, Choi EJ, Oh SP, Chen G, et al. Arteriovenous malformation in the adult mouse brain resembling the human disease. *Ann Neurol*. 2011;69:954–962. doi: 10.1002/ana.22348.

Stroke
Journal of the American Heart Association

Soluble FLT1 Gene Therapy Alleviates Brain Arteriovenous Malformation Severity

Wan Zhu, Fanxia Shen, Lei Mao, Lei Zhan, Shuai Kang, Zhengda Sun, Jeffrey Nelson, Rui Zhang, Dingquan Zou, Cameron M. McDougall, Michael T. Lawton, Thiennu H. Vu, Zhijian Wu, Abraham Scaria, Peter Colosi, John Forsayeth and Hua Su

Stroke. published online March 21, 2017;
Stroke is published by the American Heart Association, 7272 Greenville Avenue, Dallas, TX 75231

Print ISSN: 0039-2499. Online ISSN: 1524-4628

ONLINE SUPPLEMENT

Soluble FLT1 Gene Therapy Alleviates Brain Arteriovenous Malformation Severity

Supplemental Methods

Stereotactic and IV Injection of AAVs

Following isoflurane inhalation, mice were placed in a stereotactic frame (David Kopf Instruments, Tujunga, CA). A burr hole, 2 mm lateral to the sagittal suture and 1 mm posterior to the coronal suture, was drilled in the pericranium. A Hamilton syringe with 33-gauge needle was inserted 3 mm to inject 2×10^9 genome copies (gcs) of AAV1-VEGF with or without 2×10^9 gcs of AAV2-EV (empty vector) or AAV2-sFLT02 into the right basal ganglia, 0.2 µl/minute. The wound was closed with a suture.

For IV injection, AAV9-sFLT1, AAV9-GFP or AAV9-EV (1×10^{11} gcs) was injected through the left jugular vein.

Immunofluorescence Staining

Fresh-frozen brain samples were cut into 20-µm-thick coronal sections (Leica Microsystems, Wetzlar, Germany, CM1950) and stained with a rabbit anti-mouse CD31 primary antibody (Abcam, Cambridge, MA, #ab28364) and an Alex fluor 488-labeled goat anti-rabbit secondary antibody (Life Technologies, Carlsbad, CA, Cat #A-11034), and then mounted (Vectashield, Burlingame, CA, Cat #H-1500).

To double-label brain sections with CD31 and lectin, the sections were first stained with a rat anti-mouse CD31 primary antibody (Santa Cruz Biotechnology, Santa Cruz, CA, sc-18916) followed by an Alex fluor 594-labeled goat anti-rat secondary antibody (Life Technologies, Cat #A-11007), and then with a fluorescein labeled lycopersicon esculentum (Tomato) lectin (Vectashield, Cat #FL-1171). The slide was mounted (Vectashield, Cat #H-1500) after staining.

Vessel Quantification

Three images in the basal ganglia from two 20-µm-thick coronal CD 31 antibody-stained sections, 200 µm rostral and caudal of the AAV1-VEGF-injected site were captured (Keyence, Itasca, IL, model BZ-9000). Vessel density (using NIH Image J v1.63) and dysplasia vessels (manually) were quantified by three blinded researchers. Dysplasia index (DI) = number of dysplastic vessels/200 vessels.

Examination of AAV9-GFP Expression in Brain Sections

To analyze GFP expression, AAV9-GFP-injected mice were perfused with PBS through the left ventricle to wash out blood and next perfused with 4% PFA to fix the tissue and GFP protein. Brain samples were sectioned into 20-µm-thick coronal sections (Leica Microsystems, CM1950). The sections were then stained with a rabbit anti-mouse CD31 primary antibody (Abcam, #ab28364) and an Alex fluor 594-labeled goat anti-rabbit secondary antibody (Life Technologies, Cat #A-11037) and mounted (Vectashield, Cat #H-1500).

ELISA

The tissues around the bAVM lesion were collected (**Figure IID**) and lysed in a cell lysis buffer (R&D Systems, Minneapolis, MN) supplemented with PMSF (Cell Signaling, Danvers, MA, #8553). Human sFLT1 ELISA was performed using an ELISA kit (R&D Systems, DVR100B), and analyzed according to the manufacturer's instructions.

Latex Perfusion

Due to particle size, the latex cannot pass through the capillaries. After intra-left cardiac ventricle infusion, the dye enters the veins only when there are AV shunts (a key characteristic of AVM). Latex perfusion was used to detect AVM in the brain. Mice were anesthetized using isoflurane inhalation, and abdominal and thoracic cavities were opened. After cutting off the left and right atria, latex dye (blue latex, catalog BR80B; Connecticut Valley Biological Supply Co., Southampton, MA) was injected into the left ventricle using a 27-gauge needle with a 3-ml syringe.[1] Brain samples were collected, washed briefly in PBS, fixed with 10% formalin overnight, dehydrated using methanol series, and cleared with an organic solvent (benzyl alcohol/benzyl benzoate, 1:1, Sigma-Aldrich, Louis, MO).[2]

Hematoxylin and Eosin Staining

Liver tissues were fixed in 10% formaldehyde, embedded in paraffin, and cut into 5-µm-thick sections using a Leica RM 2155 microtome (Leica Microsystems). Liver sections were stained with hematoxylin and eosin using standard protocol.

Image Acquisition

Latex-perfused brain samples were frozen in dry ice after being rehydrated in PBS, and cut into 50-µm-thick coronal sections using Leica CM1950 Cryostat (Leica Microsystems). Three brain sections containing the bAVM lesion that are 500 µm apart were imaged. Total blue area (latex-perfused vessels) in the bAVM lesion in the injected hemisphere was quantified using Image J and shown as the percentage of the hemisphere's area.

Detection of Inflammatory Cells in the Liver

H&E-stained liver sections were examined and imaged using a Leica MZFL III microscope (Leica Microsystems) and Spot Insight Software (Diagnostic Instruments, Inc., Sterling Heights, MI). Ten liver sections collected from each mouse were screened, and mice that had inflammatory cell clusters were documented.

Colorimetric Assays for Alkaline Phosphatase Activity, Alanine Transaminase Activity and Creatinine Levels

After being anesthetized, approximately 100 µl of blood was collected through the facial vein, kept on ice for 30 minutes, and then centrifuged at 1,000 g for 10 minutes. Sera were collected for subsequent analyses. Alkaline phosphatase activity, alanine transaminase activity

and creatinine levels in the sera were analyzed using colorimetric assays according to the manufacturer's instructions (Abcam, #ab83369, #ab105134 and #ab65340, respectively).

Supplemental Tables

Table I. Summary of survival rate in Model 2

Treatment	# Mice	Deceased	Survival rate	Paralyzed
AAV9-GFP	22	12	43%	1
AAV9-sFLT1	19	4	76%	0

Table II. Incidence of liver inflammation in Model 1

Vectors	# Mice/group	# Mice with inflammation	Rate
AAV9-EV	5	0	0%
AAV9-GFP	12	7	58%
AAV9-sFLT1	9	5	56%

Supplemental Figures

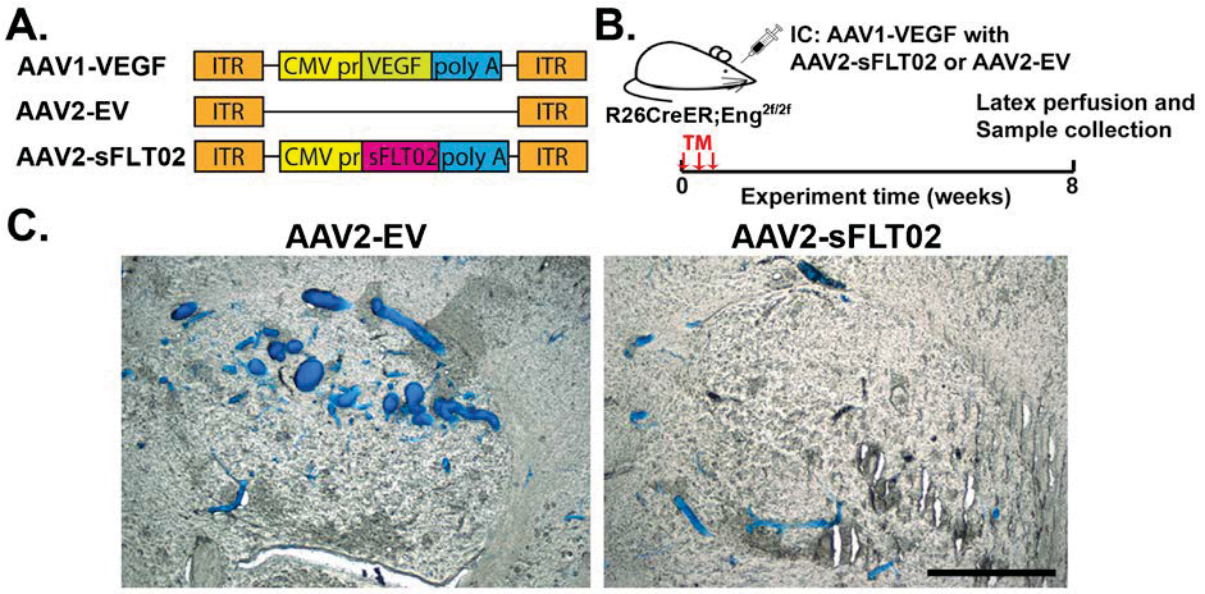

Figure I. Vector structure, treatment scheme, and representative images of latex vascular casting in the adult onset model.
(A) AAV vector structures. CMV pr: Cytomegalovirus promoter; AAV1: adeno-associated viral vector packaged in serotype 1 capsid. AAV2: adeno-associated viral packaged in serotype 2 capsid; EV: empty vector; sFLT02: the VEGF binding domain 2 of human sFLT1 and a CH3 domain of IgG1;[3] ITR: inverted terminal repeat; poly A: polyadenylation site. **(B)** Treatment scheme of intra-brain injection of AAV2-sFLT02 into R26CreER;*Eng*$^{2f/2f}$ mice. IC: intra-brain injection. TM: tamoxifen. Red arrows: Tamoxifen IP injections, three consecutive days. **(C)** Representative pictures of the basal ganglia of latex-cast brain. Scale bar: 1 mm.

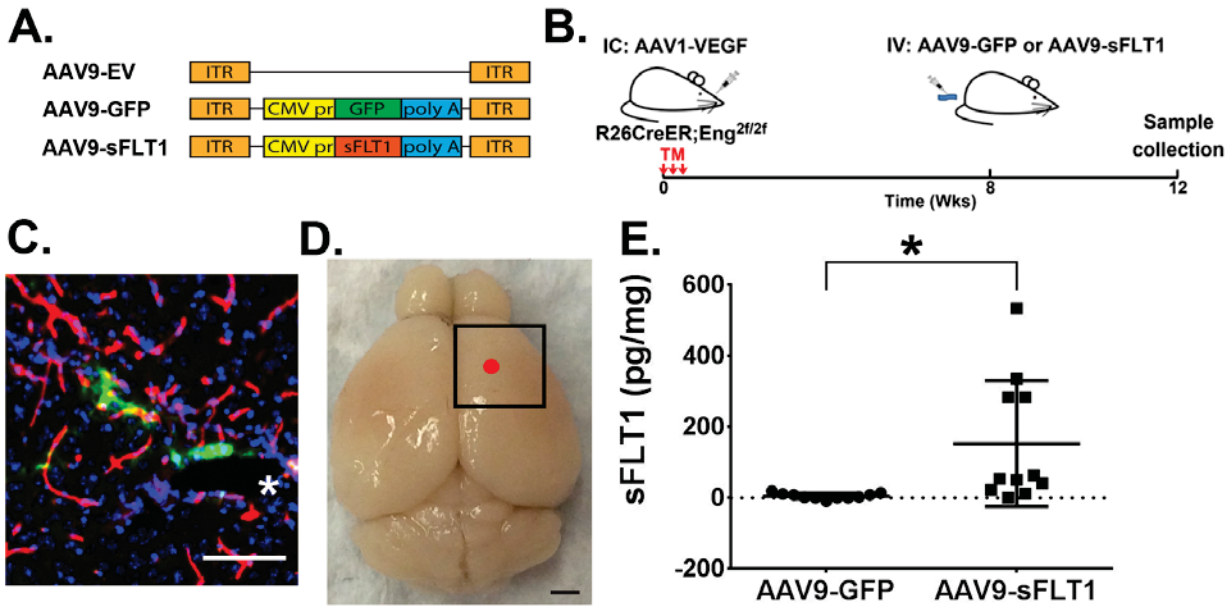

Figure II. AAV vectors for intravenous delivery, treatment scheme, and transgene expression in Model 1 mice.

(A) AAV vector structures. CMV pr: Cytomegalovirus promoter; AAV9: adeno-associated viral vector packaged in serotype 9 capsid. ITR: inverted terminal repeat; poly A: polyadenylation side. (**B**) Treatment scheme of IV injection of AAV9-sFLT1 into R26CreER;*Eng*$^{2f/2f}$ mice. IC: intra-brain injection; IV: intravenous injection; TM: tamoxifen. Red arrows: IP tamoxifen injection, three consecutive days. (**C**) GFP expression (green) in bAVM lesion. Ad-GFP-injected mice were perfused with 4% PFA before brain sample collection. Vessels were stained with a rabbit anti-CD31 antibody (red). White star indicates the lumen of a dilated vessel. The nuclei were counterstained with DAPI. Scale bar: 100 µm. **(D)** Illustration of brain region (in black rectangle) used for analysis of sFLT1 expression. Red dot indicates AAV1-VEGF injection site. Scale bar: 1 mm. **(E)** Quantification of sFLT1 expression. N=11 in each group. *: p=0.012.

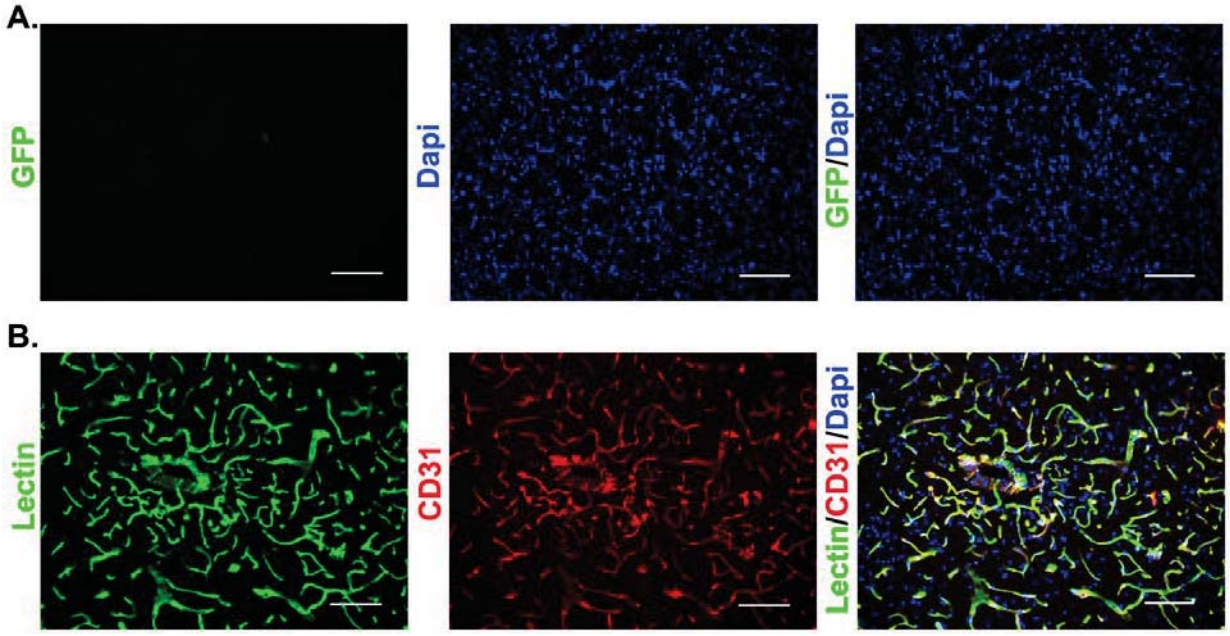

Figure III. No GFP expression present in fresh frozen brain sections of AAV9-GFP-treated mice; co-localized CD31 and lectin stains.
(A) Fresh frozen section of AD-GFP-injected brain. GFP signal was not detectable. **(B)** Lectin and CD31 positive signals were completely co-localized. Nuclei were counterstained with DAPI. Scale bars: 100 μm.

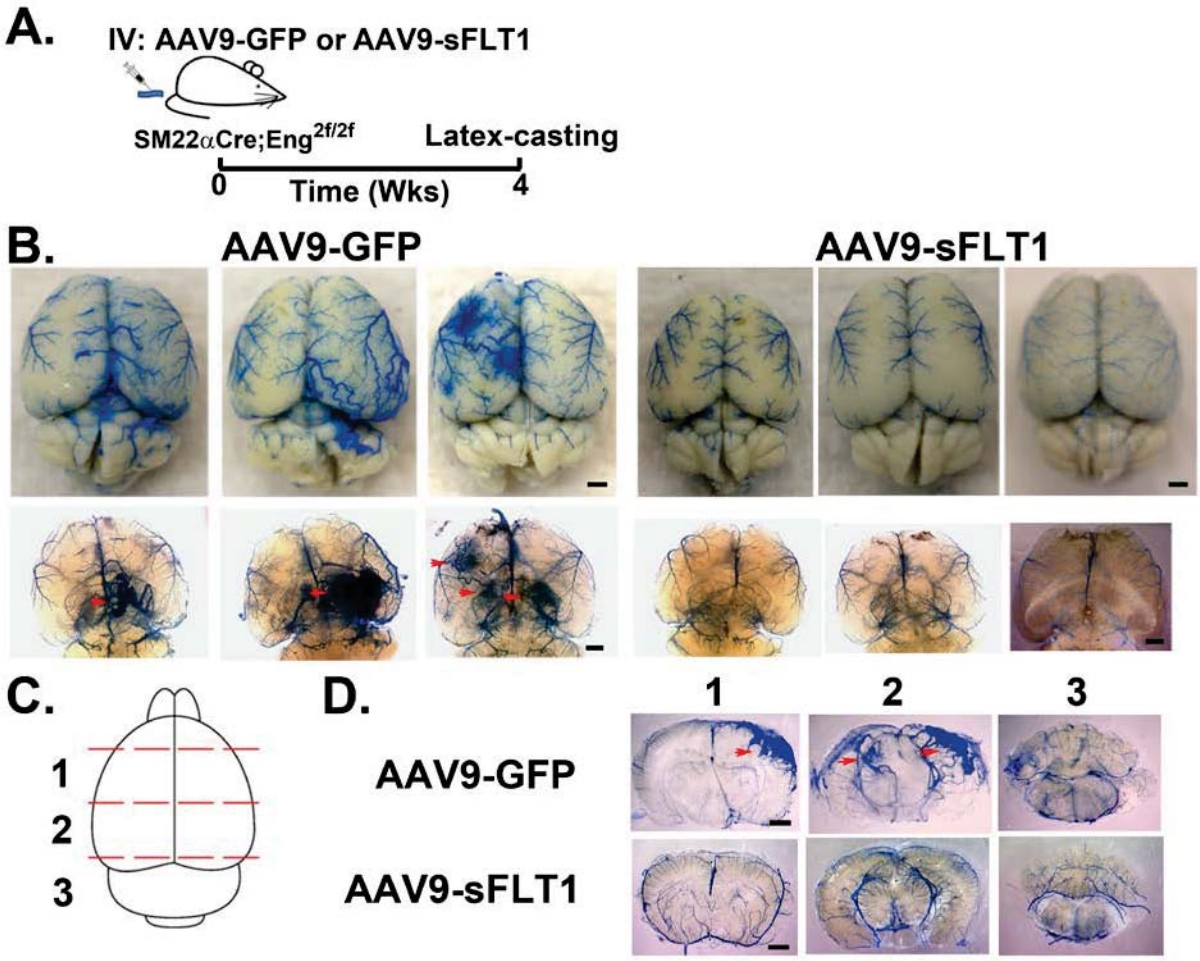

Figure IV. Treatment scheme for and additional images of AAV9-GFP- or AAV9-sFLT1-treated mice in Model 2.

(A) Treatment scheme for SM22αCre;*Eng*$^{2f/2f}$ mice. IV: intravenous injection. (**B**) Brain images of treated mice. Red arrows indicate bAVMs. Top panel shows unclarified and bottom panel shows clarified brain samples. Scale bar: 1 mm. **(C)** Illustration shows cutting lines for obtaining coronal sections shown in C. **(D)** Representative images of coronal sections. All brain samples were sectioned through the lines shown in B to examine if there was any bAVM inside the brain. Red arrows indicate bAVM. Scale bar: 1 mm.

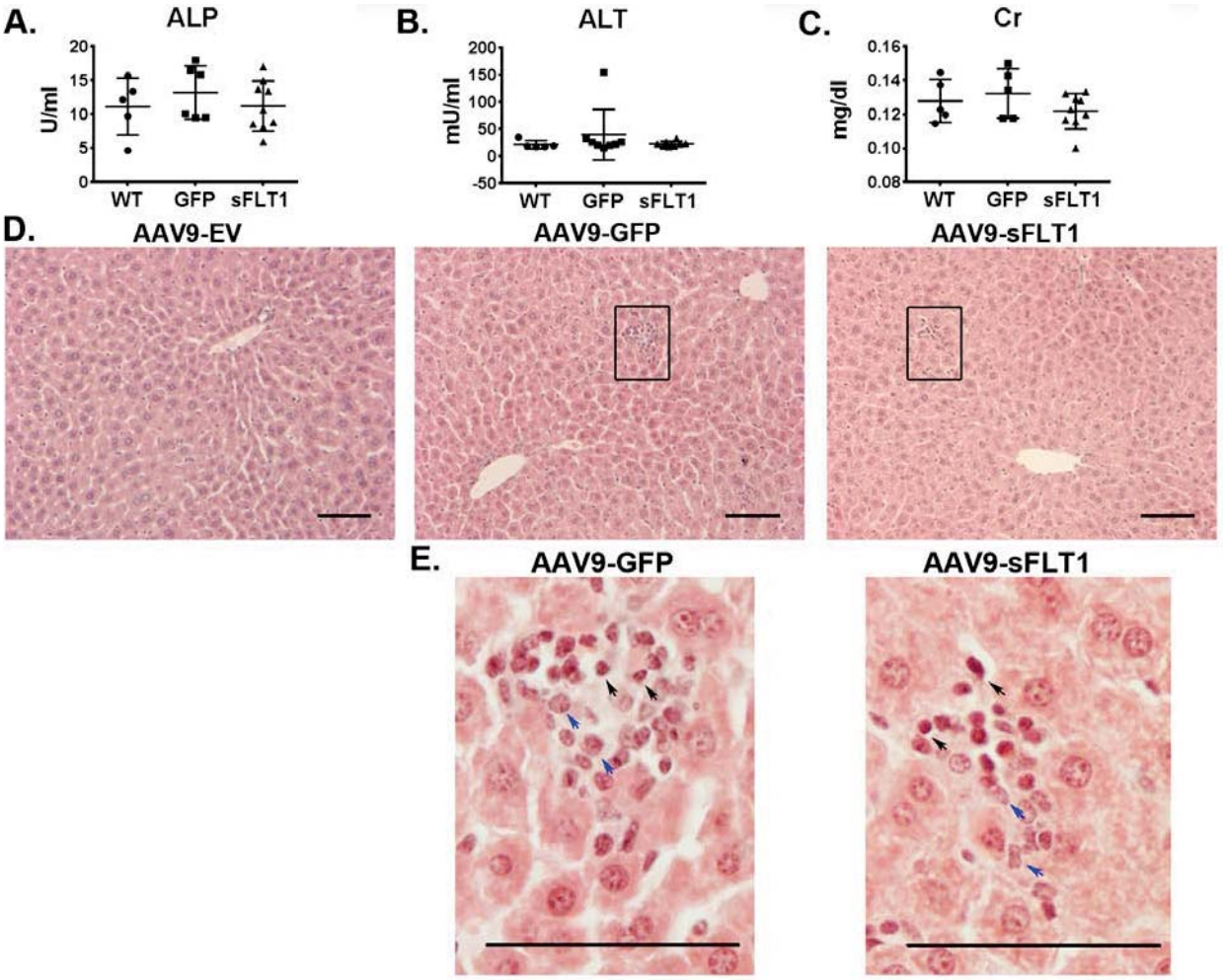

Figure V. Liver and kidney function and liver inflammation in Model 1 mice.
Quantifications of **(A)** alkaline phosphatase activity (ALP), **(B)** alanine transaminase activity (ALT), and **(C)** creatinine levels (Cr). No significant difference detected among groups. WT: untreated mice; GFP: AAV9-GFP-treated mice; sFLT1: AAV9-sFLT1-treated mice. Sample sizes: WT group: all assays used N=5; AAV9-GFP-treated: ALP assay N=6, ALT assay N=8 and Cr assay N=5; AAV9-sFLT1-treated: ALP assay N=10, ALT assay N=8, Cr assay N=9. **(D)** Representative images of H&E-stained liver sections. Small clusters of inflammatory cells were present in GFP- and sFLT1-treated mice (rectangles), similar to previous findings that expression of foreign genes can induce host immune response that may resolve over time.[4-8] (**E**) Enlarged images of rectangles in (**D**). Blue arrows and black arrows indicate monocytes and lymphocytes, respectively. Scale bar: 100 μm.

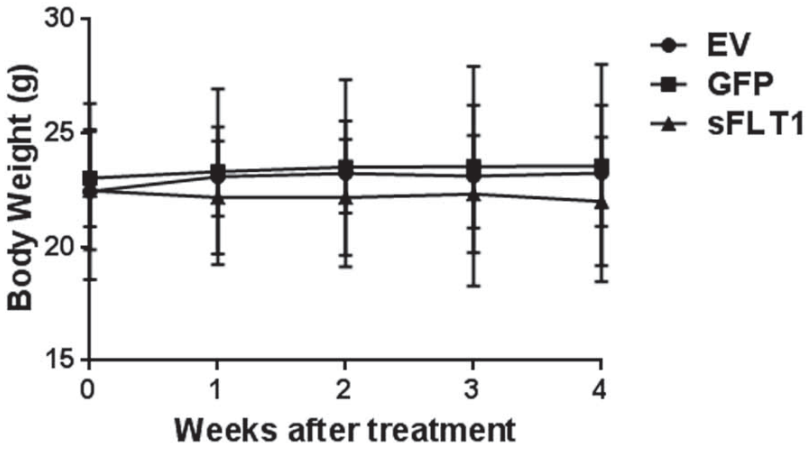

Figure VI. Changes in body weight of Model 1 mice during the therapeutic period.
Body weight was measured weekly. First measurement taken at the time vectors were injected (0). During the 4-week treatment period, the mean body weight of AAV9-sFLT1-treated mice was 22.5±2.6 g prior to the treatment, and 22.0±2.8 g (2.1% reduction) after. Body weight of AAV9-EV-treated mice increased from 22.4±3.9 g to 23.5±4.8 g (3.6% increase), and AAV9-GFP-treated mice, from 23.0±2.1 g to23.6±2.7 g (2.3% increase). N=9 for AAV9-EV group, N=15 for AAV9-GFP group and N=17 for AAV9-sFLT1 group.

Supplemental References

1. Park SO, Wankhede M, Lee YJ, Choi EJ, Fliess N, Choe SW, et al. Real-time imaging of de novo arteriovenous malformation in a mouse model of hereditary hemorrhagic telangiectasia. *J Clin Invest*. 2009;119:3487-3496.
2. Chen W, Young WL, Su H. Induction of brain arteriovenous malformation in the adult mouse. *Methods Mol Biol*. 2014;1135:309-316.
3. Pechan P, Rubin H, Lukason M, Ardinger J, DuFresne E, Hauswirth WW, et al. Novel anti-VEGF chimeric molecules delivered by AAV vectors for inhibition of retinal neovascularization. *Gene Ther*. 2009;16:10-16.
4. Gray SJ, Matagne V, Bachaboina L, Yadav S, Ojeda SR, Samulski RJ. Preclinical differences of intravascular AAV9 delivery to neurons and glia: a comparative study of adult mice and nonhuman primates. *Mol Ther*. 2011;19:1058-1069.
5. Piras BA, O'Connor DM, French BA. Systemic delivery of shRNA by AAV9 provides highly efficient knockdown of ubiquitously expressed GFP in mouse heart, but not liver. *PloS One*. 2013;8:e75894.
6. Ciesielska A, Hadaczek P, Mittermeyer G, Zhou S, Wright JF, Bankiewicz KS, et al. Cerebral infusion of AAV9 vector-encoding non-self proteins can elicit cell-mediated immune responses. *Mol Ther*. 2013;21:158-166.
7. Forsayeth J, Bankiewicz KS. Transduction of antigen-presenting cells in the brain by AAV9 warrants caution in preclinical studies. *Mol Ther*. 2015;23:612.
8. Samaranch L, San Sebastian W, Kells AP, Salegio EA, Heller G, Bringas JR, et al. AAV9-mediated expression of a non-self protein in nonhuman primate central nervous system triggers widespread neuroinflammation driven by antigen-presenting cell transduction. *Mol Ther*. 2014;22:329-337.

Stroke Online Supplement

Table I. Checklist of Methodological and Reporting Aspects for Articles Submitted to *Stroke* Involving Preclinical Experimentation

Methodological and Reporting Aspects	Description of Procedures
Experimental groups and study timeline	☒ The experimental group(s) have been clearly defined in the article, including number of animals in each experimental arm of the study. ☒ An account of the control group is provided, and number of animals in the control group has been reported. If no controls were used, the rationale has been stated. ☒ An overall study timeline is provided.
Inclusion and exclusion criteria	☐ A priori inclusion and exclusion criteria for tested animals were defined and have been reported in the article.
Randomization	☒ Animals were randomly assigned to the experimental groups. If the work being submitted does not contain multiple experimental groups, or if random assignment was not used, adequate explanations have been provided. ☐ Type and methods of randomization have been described. ☐ Methods used for allocation concealment have been reported.
Blinding	☒ Blinding procedures have been described with regard to masking of group/treatment assignment from the experimenter. The rationale for nonblinding of the experimenter has been provided, if such was not feasible. ☒ Blinding procedures have been described with regard to masking of group assignment during outcome assessment.
Sample size and power calculations	☒ Formal sample size and power calculations were conducted based on a priori determined outcome(s) and treatment effect, and the data have been reported. A formal size assessment was not conducted and a rationale has been provided.
Data reporting and statistical methods	☒ Number of animals in each group: randomized, tested, lost to follow-up, or died have been reported. If the experimentation involves repeated measurements, the number of animals assessed at each time point is provided, for all experimental groups. ☒ Baseline data on assessed outcome(s) for all experimental groups have been reported. ☒ Details on important adverse events and death of animals during the course of experimentation have been provided, for all experimental arms. ☒ Statistical methods used have been reported. ☒ Numeric data on outcomes have been provided in text, or in a tabular format with the main article or as supplementary tables, in addition to the figures.
Experimental details, ethics, and funding statements	☒ Details on experimentation including stroke model, formulation and dosage of therapeutic agent, site and route of administration, use of anesthesia and analgesia, temperature control during experimentation, and postprocedural monitoring have been described. ☒ Different sex animals have been used. If not, the reason/justification is provided. ☒ Statements on approval by ethics boards and ethical conduct of studies have been provided. ☒ Statements on funding and conflicts of interests have been provided.